Supplementary Materials: The Influence of Solar X-Ray Flares on SAR Meteorology: the Determination of the Wet Component of the Tropospheric Phase Delay and Precipitable Water Vapor

Aleksandra Nina[1,*], Jelena Radović[2], Giovanni Nico [3,4], Luka Č. Popović[5,6,7], Milan Radovanović[8,9], Pier Francesco Biagi [10] and Dejan Vinković [11]

1. X-ray flare occurred on 5 May 2010

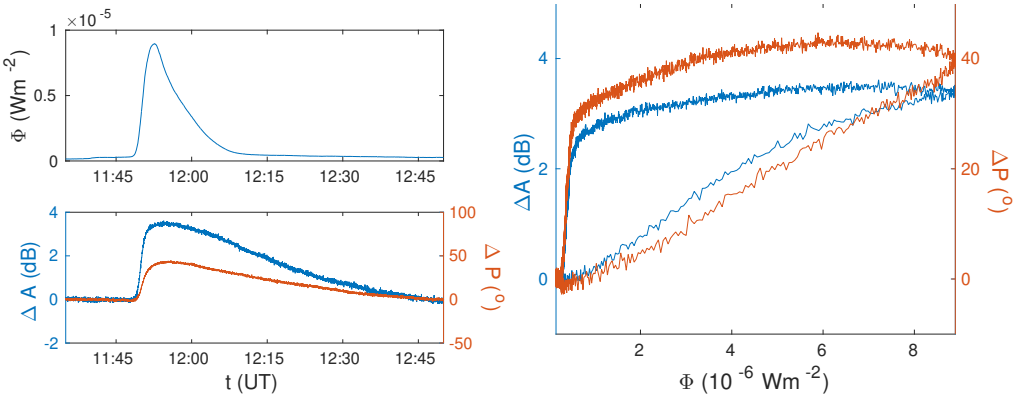

Figure S1. Upper left panel: time dependencies of the energy X-ray flux (Φ) during the flare that occurred on 5 May 2010. Bottom left panel: time dependences of the amplitude (ΔA) and phase (ΔP) changes with respect to quiet conditions. Right panel: relationships between ΔA, ΔP, and X-ray flux Φ.

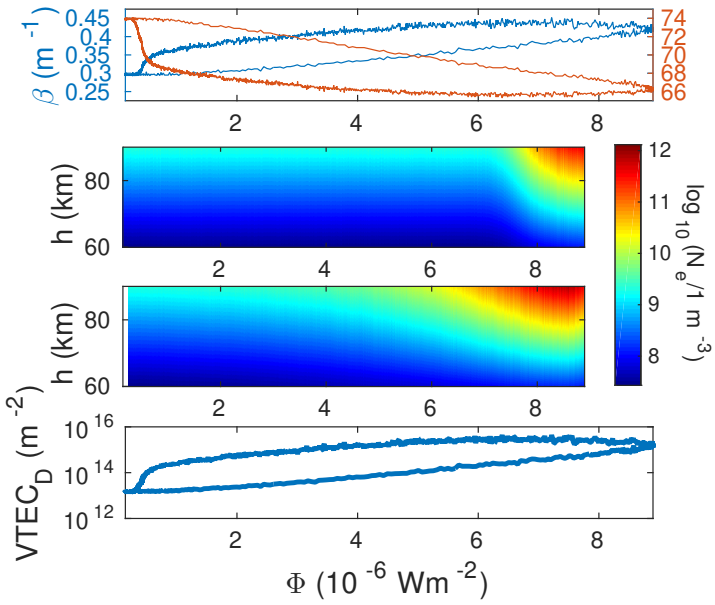

Figure S2. Dependencies of the modeled parameters on the X-ray flux (Φ) during the considered flare, which occurred on 5 May 2010. Upper panel: dependencies of Wait's parameters "sharpness" (β) and signal reflection height (H') on Φ. Middle panels: dependencies of $\log_{10}(N_e/\ 1\ \mathrm{m}^{-3})$, where N_e is the electron density given in 1 m^{-3}, before (upper middle panel) and after (bottom middle panel) the X-ray flux maximum on Φ and altitude h. Bottom panel: dependencies of the vertical total electron content in the D-region ($\mathrm{VTEC_D}$) on Φ.

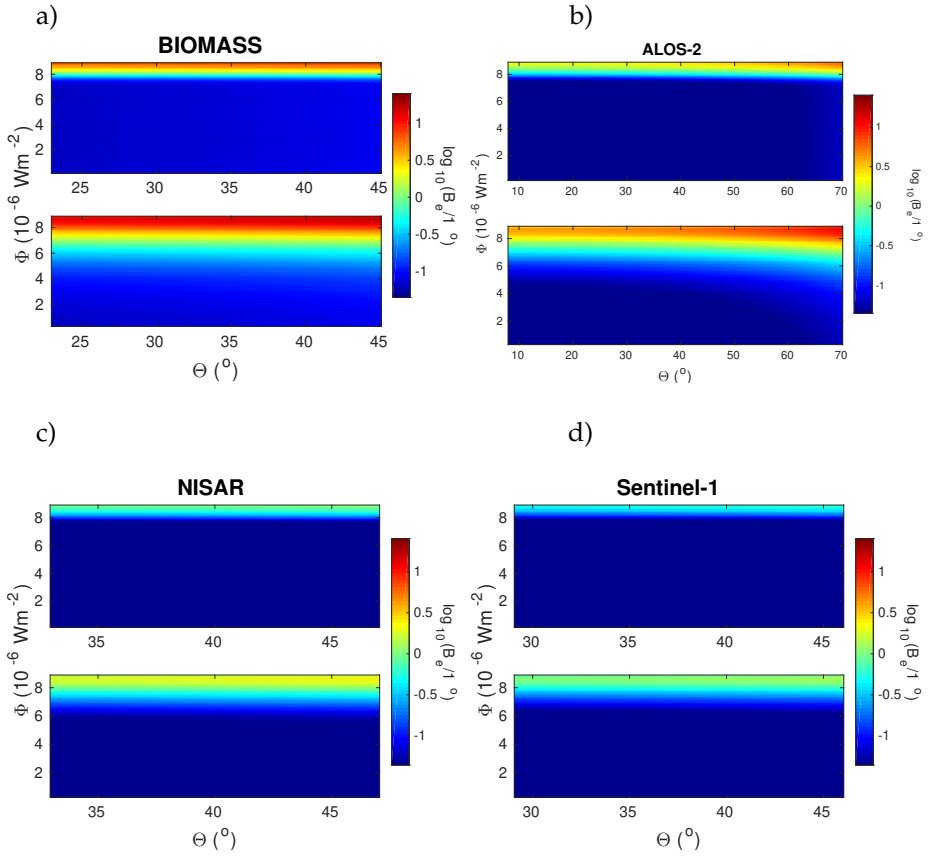

Figure S3. Dependencies of the correction factor in the determination of changes in the wet component of tropospheric phase delay (B_D) on the angle (Θ) and the X-ray flux (Φ) during the considered event for the four considered spaceborne Synthetic Aperture Radar (SAR) systems: a) BIOMASS (L-band); b) Advanced Land Observing Satellite-2 (ALOS-2) (L-band); c) National Aeronautics and Space Administration (NASA) - Indian Space Research Organisation (ISRO) Synthetic Aperture Radar (NISAR) (S-band); and d) Sentinel-1 (C-band).

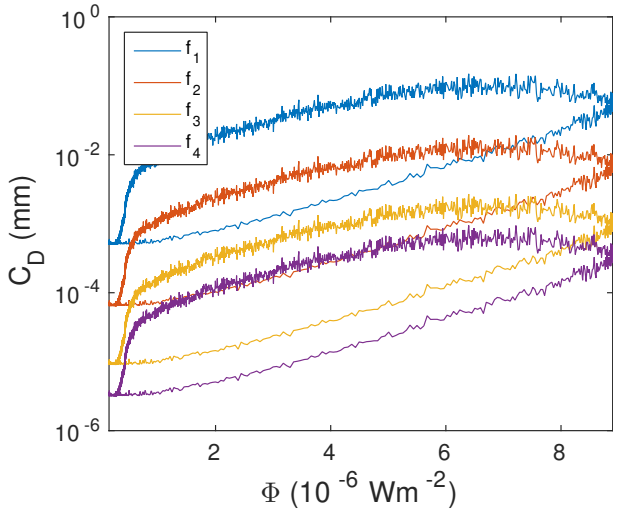

Figure S4. Dependence of the correction factor in the determination of changes in the precipitable water vapor (C_D) on the X-ray flux (Φ) during the considered event.

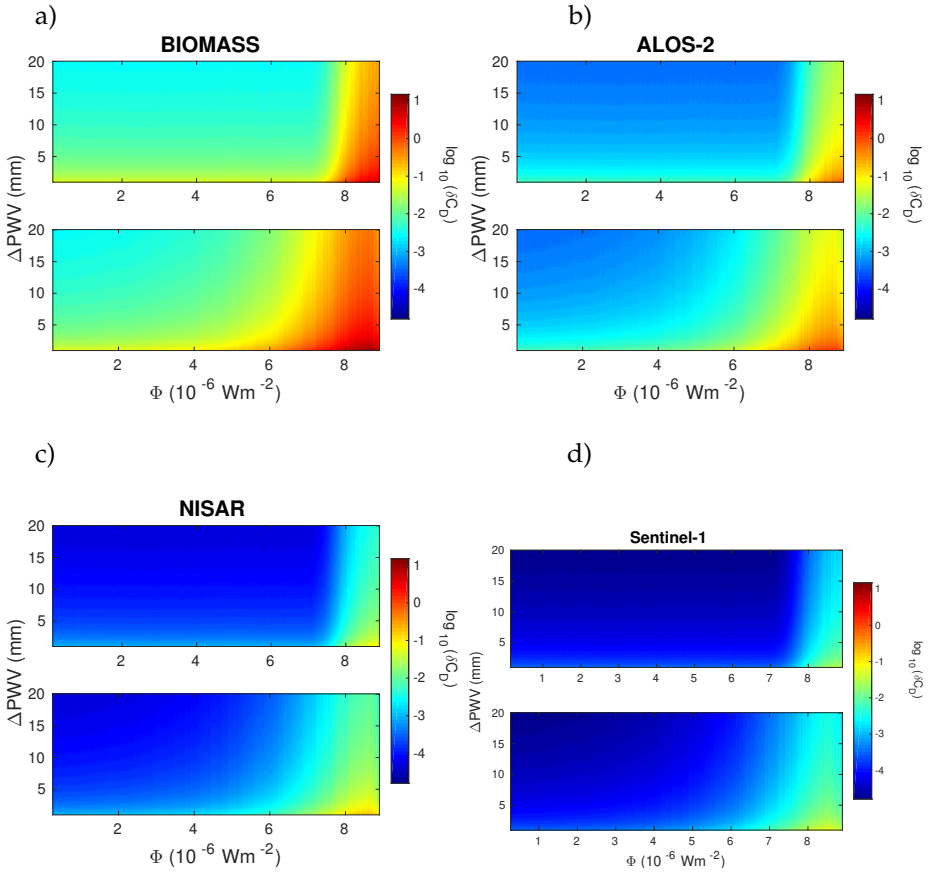

Figure S5. Dependencies of the ratio (in percent) of the correction factor in the determination of changes in the precipitable water vapor and absolute values of changes in the precipitable water vapor presented in [1] (δC_D) on the X-ray flux (Φ) and changes in the precipitable water vapor (ΔPWV) during the considered event for the four considered spaceborne Synthetic Aperture Radar (SAR) systems: a) BIOMASS (L-band), b) Advanced Land Observing Satellite-2 (ALOS-2) (L-band), c) National Aeronautics and Space Administration (NASA) - Indian Space Research Organisation (ISRO) Synthetic Aperture Radar (NISAR) (S-band) and d) Sentinel-1 (C-band).

Table 1: The maximal values of the correction factor in the determination of changes in the wet component of tropospheric phase delay (B_{Dmax}), correction factor in the determination of changes in the precipitable water vapor (C_{Dmax}), and ratio (in percent) of the correction factor in the determination of changes in the precipitable water vapor and absolute values of changes in the precipitable water vapor presented in [1] (δC_{Dmax}) during a solar X-ray flare, which occurred on 5 May 2010 for the BIOMASS, ALOS-2, NISAR, and Sentinel-1 satellites.

Satellite	B_{Dmax}	C_{Dmax}	δC_{Dmax}
BIOMASS	24.27	0.15	14.9
ALOS-2	18.06	0.019	1.9
NISAR	3.40	0.003	0.3
Sentinel-1A/B	1.98	0.0009	0.1

2. X-ray flare occurred on 8 January, 2014

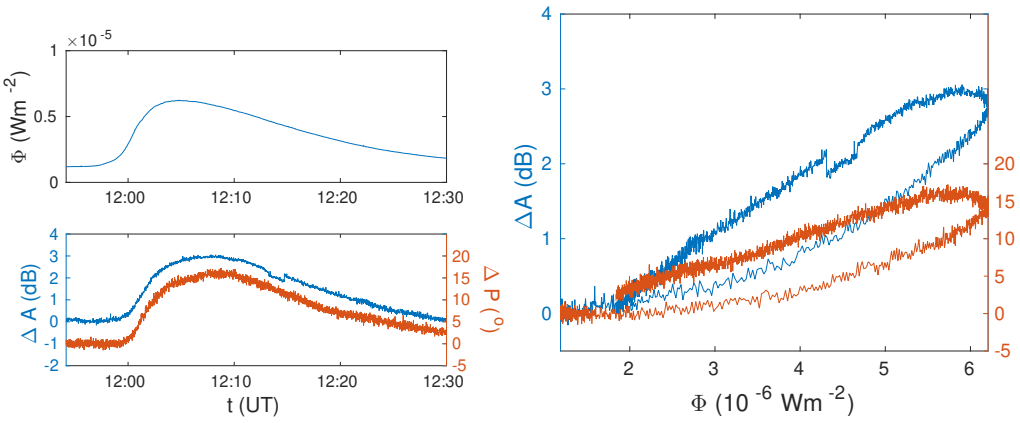

Figure S6. Upper left panel: time dependencies of the energy X-ray flux (Φ) during the flare that occurred on 8 January 2014. Bottom left panel: time dependences of the amplitude (ΔA) and phase (ΔP) changes with respect to quiet conditions. Right panel: relationships between ΔA, ΔP, and X-ray flux Φ.

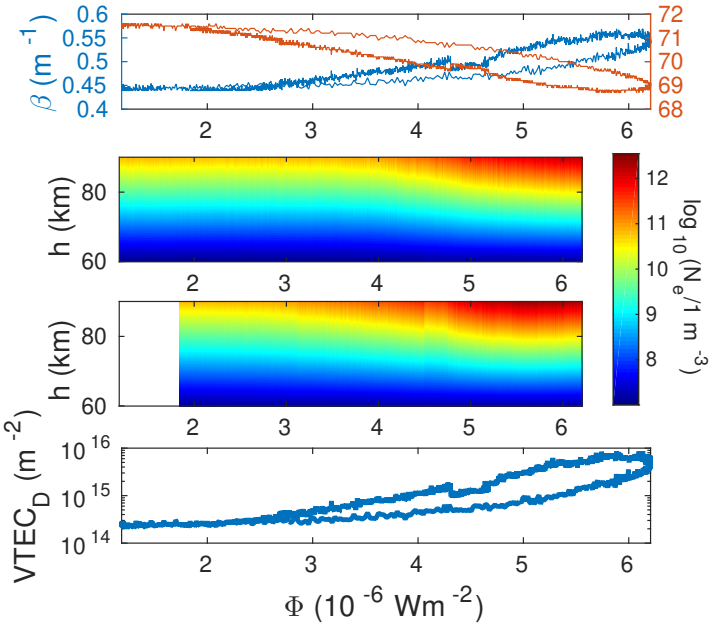

Figure S7. Dependencies of the modeled parameters on the X-ray flux (Φ) during the considered flare, which occurred on 8 January 2014. Upper panel: dependencies of Wait's parameters "sharpness" (β) and signal reflection height (H') on Φ. Middle panels: dependencies of $\log_{10}(N_e/$ 1 m^{-3}), where N_e is the electron density given in 1 m^{-3}, before (upper middle panel) and after (bottom middle panel) the X-ray flux maximum on Φ and altitude h. Bottom panel: dependencies of the vertical total electron content in the D-region (VTEC$_D$) on Φ.

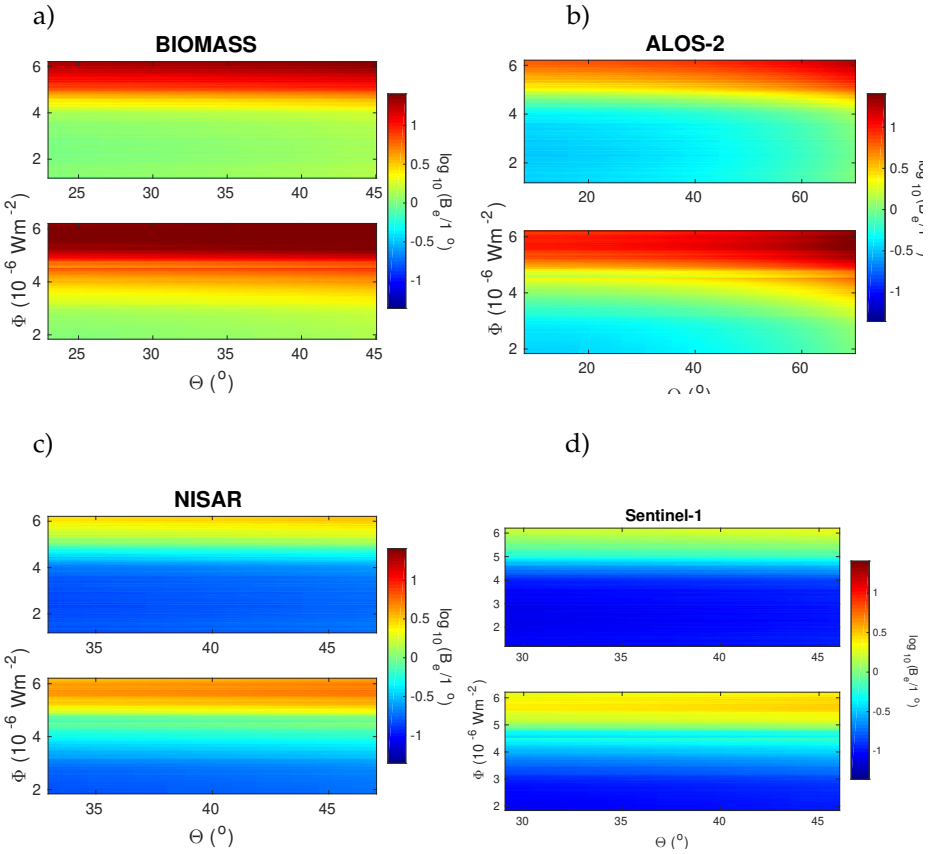

Figure S8. Dependencies of the correction factor in the determination of changes in the wet component of tropospheric phase delay (B_D) on the angle (Θ) and the X-ray flux (Φ) during the considered event for the four considered spaceborne Synthetic Aperture Radar (SAR) systems: a) BIOMASS (L-band); b) Advanced Land Observing Satellite-2 (ALOS-2) (L-band); c) National Aeronautics and Space Administration (NASA) - Indian Space Research Organisation (ISRO) Synthetic Aperture Radar (NISAR) (S-band); and d) Sentinel-1 (C-band).

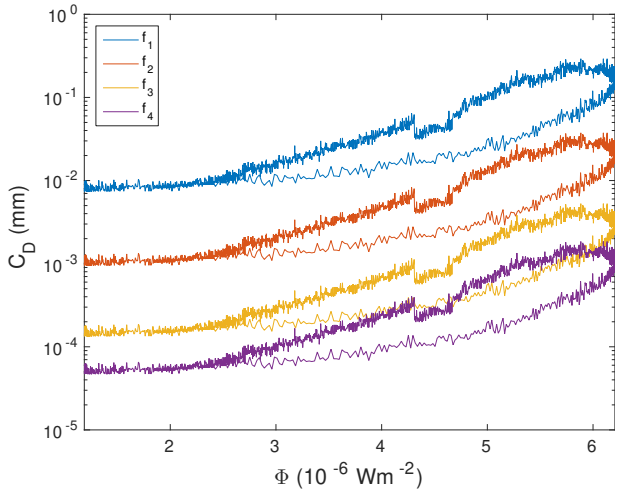

Figure S9. Dependence of the correction factor in the determination of changes in the precipitable water vapor (C_D) on the X-ray flux (Φ) during the considered event.

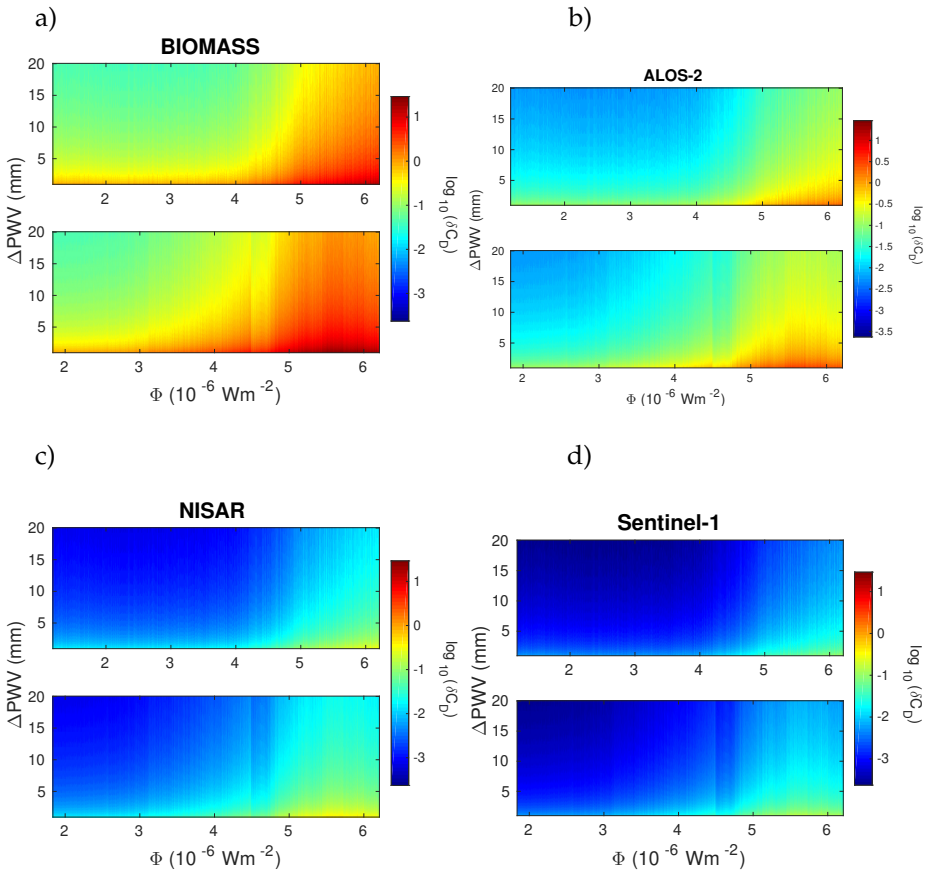

Figure S10. Dependencies of the ratio (in percent) of the correction factor in the determination of changes in the precipitable water vapor and absolute values of changes in the precipitable water vapor presented in [1] (δC_D) on the X-ray flux (Φ) and changes in the precipitable water vapor (ΔPWV) during the considered event for the four considered spaceborne Synthetic Aperture Radar (SAR) systems: a) BIOMASS (L-band), b) Advanced Land Observing Satellite-2 (ALOS-2) (L-band), c) National Aeronautics and Space Administration (NASA) - Indian Space Research Organisation (ISRO) Synthetic Aperture Radar (NISAR) (S-band) and d) Sentinel-1 (C-band).

Table 2: The maximal values of the correction factor in the determination of changes in the wet component of tropospheric phase delay (B_{Dmax}), correction factor in the determination of changes in the precipitable water vapor (C_{Dmax}), and ratio (in percent) of the correction factor in the determination of changes in the precipitable water vapor and absolute values of changes in the precipitable water vapor presented in [1] (δC_{Dmax}) during a solar X-ray flare, which occurred on 8 January 2014 for the BIOMASS, ALOS-2, NISAR, and Sentinel-1 satellites.

Satellite	B_D	C_D	δC_D
BIOMASS	47.47	0.29	29.2
ALOS-2	35.31	0.038	3.8
NISAR	6.65	0.005	0.5
Sentinel-1A/B	3.86	0.002	0.2

References

1. Mateus, P.; Catalão, J.; Nico, G. Sentinel-1 Interferometric SAR Mapping of Precipitable Water Vapor Over a Country-Spanning Area. *IEEE Trans. Geosci. Remote Sens.* **2017**, *55*, 2993–2999. doi:10.1109/TGRS.2017.2658342